Environmental Science Nano

Accepted Manuscript

ROYAL SOCIETY OF CHEMISTRY

rsc.li/es-nano

Nano Impact Statement: In addition to the fullerenes and carbon nanotubes, graphene and graphene oxide are major types of carbon-based nanomaterials. As a precursor material in the preparation of graphene, and because of its unique properties, graphene oxide (GO) likely will be used in a number of industrial and consumer products in the future. The types of products in which it will find application will partially depend on whether inclusion within these products contributes to human and environmental exposure, and the degrees of risk associated with these exposures. Because it contains many hydrophilic functional groups, it is easy to suspend in water. Hence, if released to the environment, exposure is likely to occur in aquatic environments. Yet very limited research has been conducted regarding the environmental fate of GO, its transport mechanisms in the environment, or its toxicity to aquatic species. As a result, this study investigates the photochemical reactivity of GO as it is one of the more likely fate processes acting on GO in aquatic environments. This study provides evidence that GO is chemically altered upon irradiation with solar spectrum light, and that GO serves as an electron donor, transferring electrons to molecular oxygen to form reactive oxygen species (including superoxide anion and hydrogen peroxide). This type of information is critical for assessing potential impacts of graphene oxide on aquatic environments.

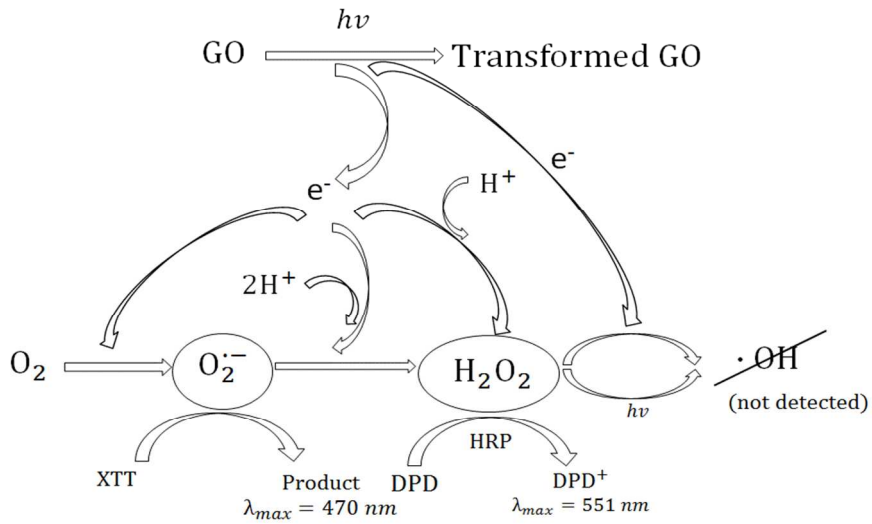

Table of Contents Entry: This study shows that $O_2^{\cdot-}$ and H_2O_2 are produced through reduction of O_2 upon solar light irradiation of aqueous graphene oxide.

Environmental Photochemistry of Single Layered Graphene Oxide in Water

Yingcan Zhao, Chad T. Jafvert*

Lyles School of Civil Engineering and Division of Environmental and Ecological Engineering, Purdue University, West Lafayette, Indiana 47907, United States

*Corresponding Author Phone: (765)494-2196; Email: jafvert@purdue.edu

Submitted to Environmental Science: Nano

Date Resubmitted: February 25, 2015

Abstract

Graphene oxide (GO) is a carbonaceous nanomaterial that is a precursor material in the preparation of graphene, and because of its unique properties, it likely will be used in a number of industrial and consumer products in the future. Despite its name, it contains many epoxy, hydroxyl, and carboxyl functional groups on its edges and surface, making it easy to suspend in water. However, how it is transformed or mineralized in natural aquatic environments, and its effects on natural processes within these environments, remain largely unknown. Therefore, in this study we report on the photochemical reactivity of single layered GO dispersed in water and irradiated with light within the solar spectrum that reaches waterbodies at earth's surface ($\lambda \geq 300$ nm). Upon irradiation, the visible color of a 5 mg/L GO suspension shifted from pale to dark brown, possibly indicating repair of some of the π bond structure; however Raman spectroscopy indicates an increase in nonaromatic defects. To further examine how oxidation or reduction on the GO surface may occur upon solar light irradiation, we probed for production of various reactive oxygen species (ROS). By monitoring ROS production with selective and highly reactive chemical probes, formation of superoxide anion ($O_2^{\cdot-}$), but not single oxygen ($^1O_2$) or hydroxyl radical (·OH), was detected, indicating electron transfer from GO to dissolved molecular oxygen (O_2). However, further electron transfer through reduction of $O_2^{\cdot-}$ did occur, as hydrogen peroxide (H_2O_2) was found to accumulate, forming 3 μM H_2O_2 in a suspension of 5 mg/L GO after 4 hours of irradiation.

Keywords: graphene oxide, reactive oxygen species, nanomaterial, ROS, environmental fate

Introduction

Many efforts are underway to discovery new ways to use graphene materials and their derivative in electronic devices, for drug delivery, in biosensors, in solar energy conversion, as catalysts, and in many other types of applications.[1-7] Due to the variety of industrial sectors in which manufactured graphene materials may find application and due to expected future production rates, release and exposure to graphene-based materials in natural and built environments may be anticipated, raising concerns over potential negative effects on human and ecosystem health if precautions are not taken to control exposure. Unfortunately, knowledge regarding the fate, transport, and toxicity of graphene and its derivatives currently is limited, especially with respect to aquatic environments. Graphene oxide (GO) is a precursor material in the preparation of graphene, and despite its name, it has on its surface several different types of functional groups, including epoxy, hydroxyl, and carboxyl groups.[8] The presence of these functional groups on GO makes it hydrophilic and easy to disperse in water.[9]

Because it is easy to disperse in water, its toxicity to human cells has been studied both as a potential aquatic pollutant, and as a potential material to selectively kill cancer cells.[6, 10] For example, Liao et al. observed that sonicated (smaller) GO exhibited greater hemolytic activity to human cells compared to larger GO materials. Viability assay experiments revealed that both graphene and GO have toxic effects to human skin fibroblasts.[11] Another research group reported that single-layer GO had dose-dependent toxicity to human lung epithelial cells and fibroblasts and caused obvious toxicity when doses were above 50 mg/L, indicating risk to human health.[12] Hu et al. found that GO could destroy cell membranes by direct interactions occurring between cell membranes and GO nanosheets.[13] In contrast, another research group used different sized GO and found that all the different sized materials showed no toxicity to A549 cells, which are typical human lung cells.[14] The variability among the results might be attributed to the various methods by which GO and graphene were produced or suspended in water. However, there is little doubt that GO might cause some toxicological effects to humans, motivating further study on the fate and effects of GO in the natural environment. Environmental effects may include toxicity to micro-organisms and other organisms up the food chain. Indeed, Akahaen et al. showed that hydrazine-reduced GO was more toxic to bacteria than the parent GO, and suggested this resulted from “sharper” nanowalls on the reduced GO (RGO).[15]

Because the disrupted π-bond structure in GO absorbs significant light within the solar spectrum, environmental fate processes acting on GO are expected to include photochemical processes. Indeed, it is well known that photo-irradiation is a good method for “reducing” GO, at least with lamp light that

occurs in UV regions that may or may not occur solely within the solar spectrum.[16] For example, in a study reporting on photo-reduction of GO conducted by Matsumoto et al.,[16] experiments were performed used a Xenon lamp of unknown spectral output, although this type of lamp generally emits light down to 280 nm, approximately 20 nm below the spectral limit of solar light measured at earth's surface. Matsumoto et al., however did measure CO_2 and H_2 generation from aqueous GO suspensions and noted a drastic decrease in H_2 production if the Xenon lamp light was filtered through a 390 nm cutoff filter. While not reported, it seems likely that a similar decrease in CO_2 production would occur under a 390 nm cutoff filter. It is somewhat interesting that while the overall reaction can be termed photo-reduction of GO, it is not clear if any of the remaining carbon on the GO has actually been reduced, as simple loss of CO_2 from carboxyl groups on GO is the result of a rearrangement reaction, where the carbon-carboxylic acid bond is broken and replaced with a carbon-hydrogen bond. Hence, although the average oxidation state of the carbon in the GO is lower, it may result from loss of carbon that was already highly oxidized, as previously reported to occur during photolysis of carboxylated multi-walled carbon nanotubes,[17] and not from any oxidation of specific carbon atoms in the GO. Similar to lack of information in the literature regarding photochemical carbonaceous products, there is a general lack of information on the generation of reactive oxygen species (ROS) by GO under solar light. Hou et al.[18] irradiated an aqueous dispersion of single layer GO with light not strictly within the solar spectrum (at energies in the range 3.94-4.43 eV; i.e., at λ = 280-315 nm), and similar to Matsumoto et al.,[16] noted that the GO became visibly darker over the irradiation period, but suggested through XPS analysis that this occurred due to loss of hydroxyl groups through hemolytic removal of ·OH groups and formation of more conjugated π-bonds, rather than through decarboxylation alone. Further, through electron paramagnetic resonance spectroscopy, dose-dependent exponential growth in radical production on the GO surface was shown to occur, presumably after loss of ·OH; however it was reported that ·OH was not observed, however the methodology of ·OH detection was not reported.

For other carbon-based nanomaterials, several reactive oxygen species have been shown to be generated under sunlight conditions (λ > 300 nm). For example, singlet oxygen ($^1O_2$) was generated in aqueous suspensions of C_{60} clusters (i.e., nano-precipitates), oxidizing the C_{60} to more polar water soluble products.[19-21] Aqueous dispersions of carboxylated and PEG-functionalized single walled carbon nanotubes (SWCNTs) produced significant ROS, including singlet oxygen ($^1O_2$), superoxide anion ($O_2^{\cdot -}$), and hydroxyl radial (·OH).[22, 23] As a result, in this study the ability of aqueous dispersions of single-layered GO to generate reactive oxygen species (ROS) upon exposure to light within solar spectrum (λ =300-410 nm) was investigated. Based on experimental results of this study and the previous work cited

above, a mechanism for ROS generation by photosensitized GO in water is proposed. Information on ROS generation during solar irradiation is significant not only to evaluate ecological risks associated with GO, but also to better understand the transformation pathways of carbon within GO.

Materials and Methods

Materials

An aqueous dispersion of single layer graphene oxide (GO), synthesized by a modified Hummer's method, was purchased from Advanced Chemical Supplier (ACS) Material, LLC (Medford, MA) and used as received. According to the manufacturer, the material is approximately 80% single-layer GO (with the remainder being multi-layered) and in the size range of 0.5 to 2.0 µm, with a thickness of 0.6 to 1.2 nm. A previous study reported the presence of phenolic hydroxyl, carboxylic, and epoxy groups within the structure of this particular graphene oxide.[24] More information on the GO material is provided in the Supporting Information (SI, **Figure SI-1**). Furfuryl alcohol (FFA), 2,3-bis(2-methoxy-4-nitro-5-sulfophenyl)-2H-tetrazolium-5-carboxanilide (XTT), *p*-chlorobenzoic acid (*p*CBA), *N,N*-diethyl-*p*-phenylenediamine hemioxalate (DPD), horseradish peroxidase (HRP), and superoxide dismutase (SOD) were purchased from Sigma-Aldrich (St. Louis, MO). All other chemicals were of the highest purity and used as received. All aqueous samples were prepared with water purified with a Barnstead Nanopure system (Dubuque, IA) after R/O pretreatment.

Preparation of Aqueous Graphene Oxide Dispersions

The stock GO dispersion (10 mg/mL) was diluted with water (1:100), and sonicated under low energy (8890R-MT ultrasonic bath from Cole-Parmer, Vernon Hills, IL) for 2 hours to make a uniform dispersion of 100 mg/L GO. When not in use, the GO suspensions were stored in the dark at room temperature. In most experiments, samples were buffered to pH 7 with a final phosphate buffer concentration of 5 mM. Buffers were prepared with phosphate salts (i.e., KH_2PO_4 and K_2HPO_4).

Irradiation and GO Analysis

For all irradiation experiments, samples were placed in a series of borosilicate glass tubes sealed with PTFE-lined caps and exposed to sixteen 24 W black-light phosphor lamps (RPR-3500Å lamps from Southern New England Ultraviolet, Branford, CT) that emit light from 300 to 400 nm, with the maximum intensity occurring near 350 nm. A figure comparing the spectral output of these lamps to that typically found for solar light at the earth's surface is provided in the SI (**Figure SI-2**). All samples were irradiated in a Rayonet merry-go-round photochemical reactor that rotated the samples at 5 rpm to ensure uniform light exposure of all samples over the irradiation period. Dark control samples were prepared

at the same time as irradiated samples and were wrapped with aluminum foil and kept in a dark environment over the same time period. All experiments were performed in duplicate or triplicate. At specific times during the irradiation period, irradiated samples and dark control samples were recovered for analysis. The UV-visible light absorbance spectra were recorded with a Varian Cary 50 UV/Vis Spectrophotometer using quartz cuvettes with 1 cm path lengths. The Raman spectra of samples were monitored by using an excitation wavelength of 633 nm, and scanning from 1000 -3000 cm^{-1} to obtain information on the characteristic D, G and 2D band intensities of GO. For all Raman spectra measurements, irradiated and dark control samples were prepared and analyzed in the absence of the phosphate buffers.

ROS Measurement

Reactive oxygen species (ROS) were detected by using specific chemical probes that selectively react with each ROS at near diffusion-limited rates. Only one probe was used at a time, as those for singlet oxygen ($^1O_2$) superoxide anion ($O_2^{\cdot-}$), and hydroxyl radical (·OH) require that they be added before the irradiation period, as the measured response is due to accumulative ROS production; whereas analysis of hydrogen peroxide (H_2O_2) was performed on samples by adding the necessary reagents after irradiation. $^1O_2$ was monitored by the loss of FFA.[25] Detailed information about detecting $^1O_2$ with FFA is included in the SI. Previously, we used a nitro blue tetrazolium salt (referred to as NBT^{2+}) as a scavenger for $O_2^{\cdot-}$ that was produced upon solar light irradiation of functionalized carbon nanotubes (CNTs).[22] However, in the presence of NBT^{2+}, GO was found to flocculate and settle; hence experiments using XTT as a scavenging probe for $O_2^{\cdot-}$ were attempted with success. The reaction between XTT and $O_2^{\cdot-}$ leads to a soluble product that was detected spectrophotometrically at 470 nm after filtering samples through 0.2 µm membrane filters to remove the GO, which also absorbs light at 470 nm. To confirm that transformation of XTT was through reaction with $O_2^{\cdot-}$, in some GO + XTT samples, superoxide dismutase (SOD) was added, as it significantly decreases the steady-state concentration of $O_2^{\cdot-}$ by enzymatically catalyzing its disproportionation to hydrogen peroxide (H_2O_2), confirming transformation of XTT was due to reaction with $O_2^{\cdot-}$. *p*-Chlorobenzoic acid (*p*CBA) was added to some samples to determine if ·OH was generated during irradiation.[22] *p*CBA reacts rapidly with ·OH resulting in loss of *p*CBA from the system; The complete *p*CBA method is described in the SI. H_2O_2 temporal concentrations were measured by horseradish peroxidase (HRP) catalyzed oxidation of DPD, with the HRP and DPD added to samples after irradiation or incubation in the dark.[26, 27] Before analyzing samples for H_2O_2, irradiated and dark control samples were filtered through 0.2 µm membrane filters to remove the GO, which otherwise would interfere with DPD spectrophotometric detection. After filtration, 1 mL of each sample was added to 1

mL phosphate buffer (pH 6), followed sequentially by additions of 50 µL 30 mM DPD solution and 50 µL 30 U/mL HRP. H_2O_2 concentrations were determined by comparing sample absorbances at 551 nm to that of known standards (i.e., from a standard curve).

Results and Discussion

Upon irradiation of an aqueous dispersion of single layered GO with light in the solar spectrum, the GO dispersion become visibly darker as shown in **Figure 1a**. This is consistent with previous observations noted in the introduction section that reported on exposure of GO to shorter wavelength UV light.[16, 18] Similarly, light attenuation (**Figure 1b**) of the GO suspension increased across the whole spectrum from 220 to 820 nm. Note that although the figure reports "absorbance", the response is due to both light absorbance and scatter because the samples are nanoparticle suspensions that not only absorb light within this wavelength range, but also scatter the light, with presumably much of the light attenuation at the higher wavelengths occurring due to light scattering. The GO spectra before irradiation does exhibit two characteristic peaks: A maximum at approximately 230 nm, which corresponds to $\pi \rightarrow \pi^*$ transitions of the aromatic C–C bonds, and a shoulder at 303 nm, which is due to $n \rightarrow \pi^*$ transitions of C=O bonds.[28] Over the course of a 2 hr irradiation period, the absorption peak at 230 nm was gradually red-shifted to approximate 255 nm and the shoulder at 303 nm disappeared, potentially indicating that some of the electronic conjugation within the graphene sheets was restored as previously suggest upon reduction of GO with light at shorter wavelengths.[18, 29]

Raman spectroscopy is often used to probe differences in the electronic properties of carbon nanomaterials.[30] **Figure 2** shows the Raman spectral changes in GO as a function of irradiation time. The spectra shows the D, G, and 2D bands, which are three characteristic peaks of GO. The G band occurs at 1580 cm^{-1} and results from the vibration of sp^2-bonded carbon, and is an indication of the relative extent of aromaticity. The D band at 1350 cm^{-1} is assigned to the vibration of sp^3 carbon atoms (i.e., nonaromatic carbon). The relative intensities, or ratio of the D to G band intensities (I_D/I_G) is often used as a qualitative measure for the degree of disorder caused by nonaromatic sp^3 carbon defects, that often occur at edges or as ripples or holes within the GO structure.[31] **Figure 2** shows that after 24 hrs of irradiation, the I_D/I_G ratio increased from 0.45 (0 hr) to 0.68 (24 hr). This increase suggests an increase in the number of defects (e.g., functionalized carbon) on the already functionalized graphene oxide sheets. These defects may be sites for ROS production, which is discussed subsequently.

By monitoring ROS production with the selective and highly reactive chemical probes, formation of $O_2^{\cdot-}$, but not $^1O_2$ or ·OH, was detected. Irradiated samples containing furfuryl alcohol as a scavenging

probe for $^1O_2$, showed no decay in furfuryl alcohol after 24 hrs of irradiation (**Figure SI-3**). However, in GO suspensions containing XTT, a significance increase in light absorbance at 470 nm occurred over time upon irradiation and after filtering out the GO after irradiation. This increase in absorbance occurs where the reaction product between XTT and $O_2^{\cdot-}$ has an absorbance maximum[22] (**Figure 3**). **Figure 3a** also indicates that the addition of SOD almost completely inhibited XTT reduction, further suggesting that XTT product formation was caused directly by reaction of XTT with $O_2^{\cdot-}$ as SOD rapidly converts $O_2^{\cdot-}$ to H_2O_2 through a disproportionation reaction, reducing the amount of XTT product formed. In the absence of XTT, irradiated and dark control GO samples showed little change in absorbance at 470 nm over the same time period. Note that because the light absorption spectral changes shown in Figure 3B (and reported at 470 nm in Figure 3A) are on samples filtered through 0.2 μm membrane filters (i.e, after removal of GO), the increase in absorbance at 470 was due only to XTT product formation and not due to the increase in light absorbance caused by the GO, as shown in **Figure 1** on unfiltered samples. An image showing the course of the reaction from 0 to 3 hours for a 5 mg/L GO suspension containing 0.1 mM XTT, prior to filtration, is provided in the SI (**Figure SI-4**). Even with the increase in overall absorbance caused by the GO, the pink product of reaction between $O_2^{\cdot-}$ and XTT is evident.

With significant $O_2^{\cdot-}$ formation, there is a high probability that hydrogen peroxide will form also, and potentially accumulate in solution. As noted above, H_2O_2 can be formed by the disproportionation of $O_2^{\cdot-}$ with enzymes such as SOD accelerating the rate of the reaction considerably. As the disproportionation reaction suggests, conversion can occur also through transfer of another electron to the protonated form of superoxide anion, $HO_2^{\cdot}$ (hydroperoxyl radical), which upon the electron transfer, extracts a proton from solution to form H_2O_2. Whether it occurs by disproportionation or another electron transfer process, both electrons must originate from the GO in the absence of an additional electron donor. Hence, accumulation of H_2O_2 was measured by using the DPD-horseradish peroxidase (HRP) assay, with the DPD/HRP added to the aqueous samples after irradiating the GO dispersions, and then after removing the GO by filtration. Although H_2O_2 is somewhat reactive in this system, it has a much longer half-live that the other ROS, even under solar light irradiation. **Figure 4a** clearly shows that the H_2O_2 concentration within the GO dispersions increased over an irradiation period of 4 hrs, whereas no increase occurred in dark control samples or in the absence of GO. The H_2O_2 concentrations shown on **Figure 4a** were calculated from sample absorbance valued measured at 551 nm after filtration, using the H_2O_2 standard curve shown on **Figure 4b**. Hence, the initial values at time zero of 0.2-0.5 μM are due to absorbance reading at or below 0.005, and likely due to trace contamination resulting in a small positive interference. Despite this, the results indicate that H_2O_2 was indeed produced and accumulated

during irradiation of 5 mg/L GO with light in the solar spectrum, accumulating to over 3 μM after an irradiation period of 4 hrs. Assuming a carbon content of 80% in the original GO, the 5 mg/L GO concentration translates to a molar concentration of 3 mM carbon. Hence, over the 4 hr irradiation period, approximately 1 molecule of H_2O_2 was produced for every 1,000 carbon atoms in the GO.

Although it is known that sunlight can cleave the oxygen-oxygen bond in H_2O_2 to form ·OH, the reaction is slow.[23, 32] Alternatively, ·OH may be formed more rapidly if transfer of an addition electron from GO to H_2O_2 occurs, as was found to be the case for carboxylated single walled carbon nanotubes under solar irradiation.[23] In order to determine whether there is hydroxyl radical produced by GO, *p*CBA was added to some samples, as it rapidly scavenges ·OH resulting in loss of *p*CBA. However, no *p*CBA decay was observed for both irradiated and dark control samples over the 4 hour time period of the experiments (see the SI, **Figure SI-5**), suggesting that negligible ·OH was produced, or that ·OH scavenging by the GO was rapid and significant, reducing its pseudo-steady-state concentration. Although scavenging of ·OH by GO is likely to occur, as the initial electron transfer that results in its formation would occur at the GO surface such that the site of its generation would be in close proximity to GO π bonds at which it could be consumed, it is also likely that not much is produced, otherwise the concentration of its precursor, H_2O_2 would not accumulate to such a degree, and the chromophore content of the GO would not become enhanced as irradiation proceeds.

Conclusions

In summary, when exposed to light within the solar spectrum, aqueous dispersions of single layered GO do become darker, indicating an increase in chromophore content, or at least an increasing absorptivity by the existing chromophores within GO, yet Raman spectroscopy indicates an increase in nonaromatic defects. Clearly, upon exposure to light, electron transfer occurs from GO to O_2, forming $O_2^{\cdot-}$ and significant quantities of H_2O_2 as depicted in Scheme 1, and because these are both reduction reactions, this must result in an overall oxidation of GO carbon. Although it is likely that some of the generated ROS reacts directly with the GO surface, this clearly does not occur stoichiometrically, as evidenced by the buildup in the H_2O_2 concentration over a time period of several hours. These results suggest that future studies should examine whether these electron transfer reactions are responsible for some of the toxicological effects observed for GO. In a recent study[27] we report that electrons from common biological reducing agents (i.e., NADH) can be shuttled through single-walled carbon nanotubes to molecular oxygen in the dark, resulting in ROS production and DNA cleavage. It is likely that a similar

mechanism resulting in oxidative stress may occur also in the case of GO, but this hypothesis is yet to be tested.

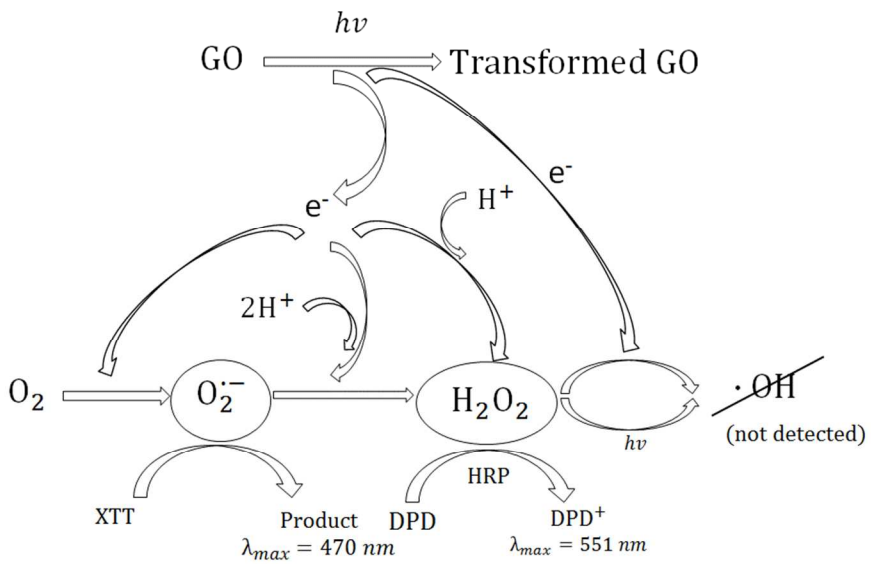

Scheme 1. Proposed pathway for ROS production by photosensitization of GO in water.

Acknowledgements

This research was supported by the United States Environmental Protection Agency (U.S. EPA) STAR Grant Program (Grant No. RD 83485801). We also acknowledge and thank the support of the China Scholarship Council (CSC) through a Ph.D. fellowship awarded to Yingcan Zhao to study at Purdue University. Presented at the 9th International Conference on the Environmental Effects of Nanoparticles and Nanomaterials, South Carolina, USA, September 2014.

Supporting Information available

Additional information as mentioned in the text is available free of charge with the electronic version of this paper at http://www.rsc.org.

References

1 A. K. Geim, K. S. Novoselov, *Nature materials* **2007**, *6*, 183-191.
2 A. K. Geim, *science* **2009**, *324*, 1530-1534.
3 J. H. Jung, D. S. Cheon, F. Liu, K. B. Lee, T. S. Seo, *Angewandte Chemie International Edition* **2010**, *49*, 5708-5711.
4 I. V. Lightcap, T. H. Kosel, P. V. Kamat, *Nano letters* **2010**, *10*, 577-583.
5 Y. Song, K. Qu, C. Zhao, J. Ren, X. Qu, *Advanced Materials* **2010**, *22*, 2206-2210.

6 X. Sun, Z. Liu, K. Welsher, J. T. Robinson, A. Goodwin, S. Zaric, H. Dai, *Nano research* **2008**, *1*, 203-212.
7 X. Wang, L. Zhi, K. Müllen, *Nano letters* **2008**, *8*, 323-327.
8 D. R. Dreyer, S. Park, C. W. Bielawski, R. S. Ruoff, *Chemical Society Reviews* **2010**, *39*, 228-240.
9 F. Barroso-Bujans, S. Cerveny, R. Verdejo, J. del Val, J. Alberdi, A. Alegría, J. Colmenero, *Carbon* **2010**, *48*, 1079-1087.
10 K. Yang, J. Wan, S. Zhang, B. Tian, Y. Zhang, Z. Liu, *Biomaterials* **2012**, *33*, 2206-2214.
11 K.-H. Liao, Y.-S. Lin, C. W. Macosko, C. L. Haynes, *ACS applied materials & interfaces* **2011**, *3*, 2607-2615.
12 K. Wang, J. Ruan, H. Song, J. Zhang, Y. Wo, S. Guo, D. Cui, *Nanoscale Res Lett* **2011**, *6*.
13 W. Hu, C. Peng, M. Lv, X. Li, Y. Zhang, N. Chen, C. Fan, Q. Huang, *Acs Nano* **2011**, *5*, 3693-3700.
14 Y. Chang, S.-T. Yang, J.-H. Liu, E. Dong, Y. Wang, A. Cao, Y. Liu, H. Wang, *Toxicology letters* **2011**, *200*, 201-210.
15 O. Akhavan, E. Ghaderi, *Acs Nano* **2010**, *4*, 5731-5736.
16 Y. Matsumoto, M. Koinuma, S. Ida, S. Hayami, T. Taniguchi, K. Hatakeyama, H. Tateishi, Y. Watanabe, S. Amano, *The Journal of Physical Chemistry C* **2011**, *115*, 19280-19286.
17 J. L. Bitter, J. Yang, S. BeigzadehMilani, C. T. Jafvert, D. H. Fairbrother, *Environ. Sci. Nano* **2014**, *1*.
18 X.-L. Hou, J.-L. Li, S. C. Drew, B. Tang, L. Sun, X.-G. Wang, *The Journal of Physical Chemistry C* **2013**, *117*, 6788-6793.
19 W.-C. Hou, C. T. Jafvert, *Environmental science & technology* **2008**, *43*, 362-367.
20 W.-C. Hou, C. T. Jafvert, *Environmental science & technology* **2009**, *43*, 5257-5262.
21 W.-C. Hou, L. Kong, K. A. Wepasnick, R. G. Zepp, D. H. Fairbrother, C. T. Jafvert, *Environmental science & technology* **2010**, *44*, 8121-8127.
22 C.-Y. Chen, C. T. Jafvert, *Environmental science & technology* **2010**, *44*, 6674-6679.
23 C.-Y. Chen, C. T. Jafvert, *Carbon* **2011**, *49*, 5099-5106.
24 H. Chen, B. Gao, H. Li, *Journal of hazardous materials* **2015**, *282*, 201-207.
25 W. R. Haag, J. Hoigne, *Environmental science & technology* **1986**, *20*, 341-348.
26 H. Bader, V. Sturzenegger, J. Hoigne, *Water Research* **1988**, *22*, 1109-1115.
27 H.-S. Hsieh, R. Wu, C. T. Jafvert, *Environmental science & technology* **2014**, *48*, 11330-11336.
28 J. Paredes, S. Villar-Rodil, A. Martinez-Alonso, J. Tascon, *Langmuir* **2008**, *24*, 10560-10564.
29 J. G. Radich, P. V. Kamat, *ACS nano* **2013**, *7*, 5546-5557.
30 M. S. Dresselhaus, A. Jorio, M. Hofmann, G. Dresselhaus, R. Saito, *Nano letters* **2010**, *10*, 751-758.
31 G. Eda, M. Chhowalla, *Advanced Materials* **2010**, *22*, 2392-2415.
32 W.-C. Hou, S. BeigzadehMilani, C. T. Jafvert, R. G. Zepp, *Environ. Sci. Technol.* **2014**, *48*, 3875-3882.

List of Figures

Figure 1. (a) Photograph of 5 mg/L GO at pH 7, before (left vial) and after (right vial) irradiation for 2 hours with lamps that emit light from 300 to 410 nm; and (b) the change in the UV-visible light absorption spectra of similar GO suspensions with increasing time of irradiation.

Figure 2. The Raman spectra of GO before and after irradiating an aqueous GO suspension (100 mg/L) for 24 hours, where the spectra have been normalized to the intensity of the G band.

Figure 3. (a) Evidence of $O_2^{\cdot-}$ formation by reaction with XTT, forming the pink colored reduction product that absorbs light at λ_{max} = 470 nm, upon lamp light irradiation of a 5 mg/L GO suspension at pH 7. The symbols represent samples containing XTT (0.1 mM) alone (▲); GO (5 mg/L) alone (♦); GO (5 mg/L) and XTT (0.1 mM) (■); GO (5 mg/L), XTT (0.1 mM) and SOD (40 U/mL) (●); and the corresponding dark control samples of GO (5 mg/L) and XTT (0.1 mM) (□). (b) The change in the UV-visible light absorption spectra for a suspension of GO (5 mg/L) and XTT (0.1 mM) as a function of irradiation time, after filtering the samples through 0.2 µm filters to remove the GO.

Figure 4. (a) Evidence for the increase in H_2O_2 concentration over time upon lamp light irradiation of GO at pH 7, by reacting the accumulated H_2O_2 with DPD through the HRP catalyzed reaction, producing the red colored DPD Würster dye product that absorbs light at 551 nm. All samples contain DPD and HRP, added after irradiating samples which contained 5 mg/L GO (■), or pure water (▲), or after incubating samples in the dark which contained 5 mg/L GO (□); and with the DPD and HRP added after filtering out the GO through 0.2 µm membrane filters. (b) The standard curve of H_2O_2 using DPD/HRP method.

(a)

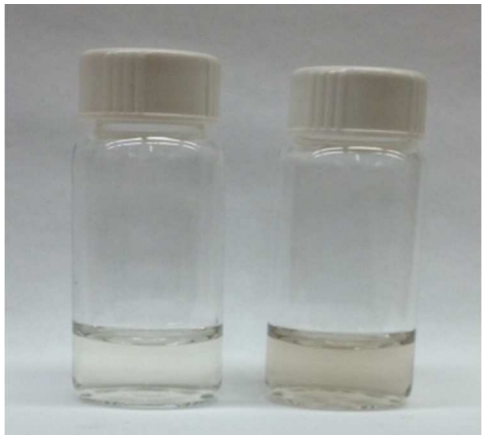

(b)

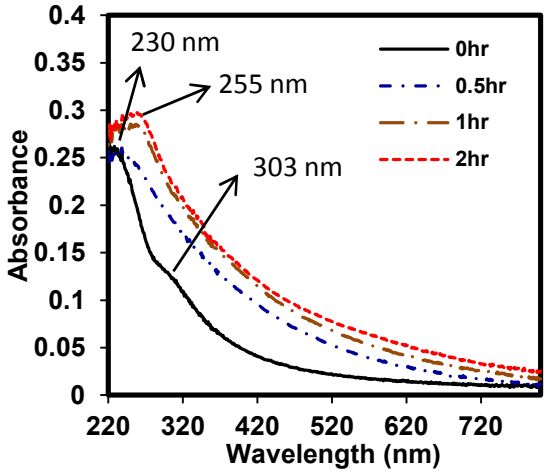

Figure 1. (a) Photograph of 5 mg/L GO at pH 7, before (left vial) and after (right vial) irradiation for 2 hours with lamps that emit light from 300 to 410 nm; and (b) the change in the UV-visible light absorption spectra of similar GO suspensions with increasing time of irradiation.

342
343
344
345
346
347
348
349
350
351

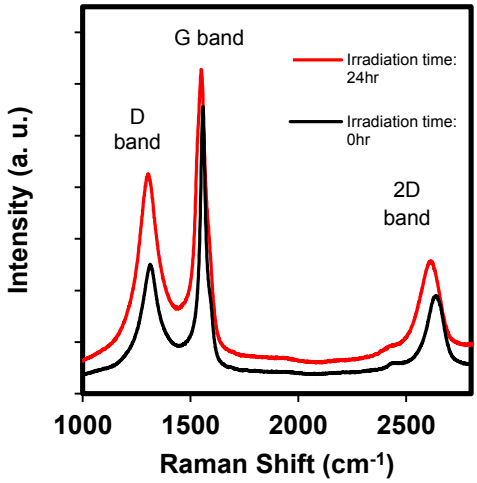

Figure 2. The Raman spectra of GO before and after irradiating an aqueous GO suspension (100 mg/L) for 24 hours, where the spectra have been normalized to the intensity of the G band.

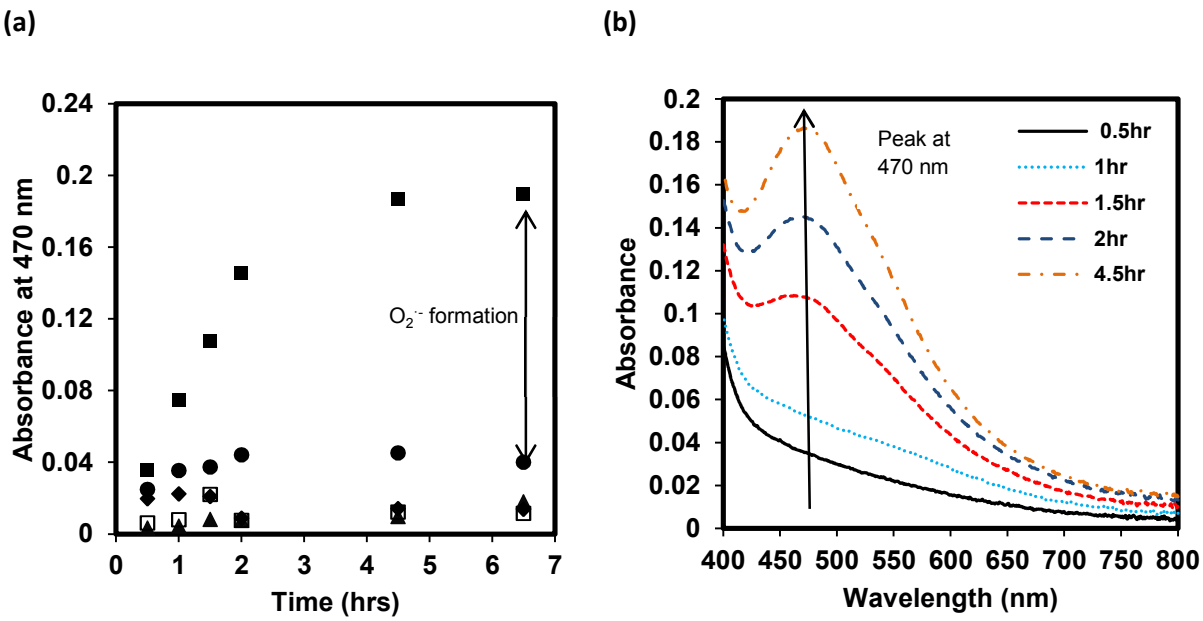

Figure 3. (a) Evidence of $O_2^{\cdot-}$ formation by reaction with XTT, forming the pink colored reduction product that absorbs light at λ_{max} = 470 nm, upon lamp light irradiation of a 5 mg/L GO suspension at pH 7. The symbols represent samples containing XTT (0.1 mM) alone (▲); GO (5 mg/L) alone (♦); GO (5 mg/L) and XTT (0.1 mM) (■); GO (5 mg/L), XTT (0.1 mM) and SOD (40 U/mL) (●); and the corresponding dark control samples of GO (5 mg/L) and XTT (0.1 mM) (□). (b) The change in the UV-visible light absorption spectra for a suspension of GO (5 mg/L) and XTT (0.1 mM) as a function of irradiation time, after filtering the samples through 0.2 µm filters to remove the GO.

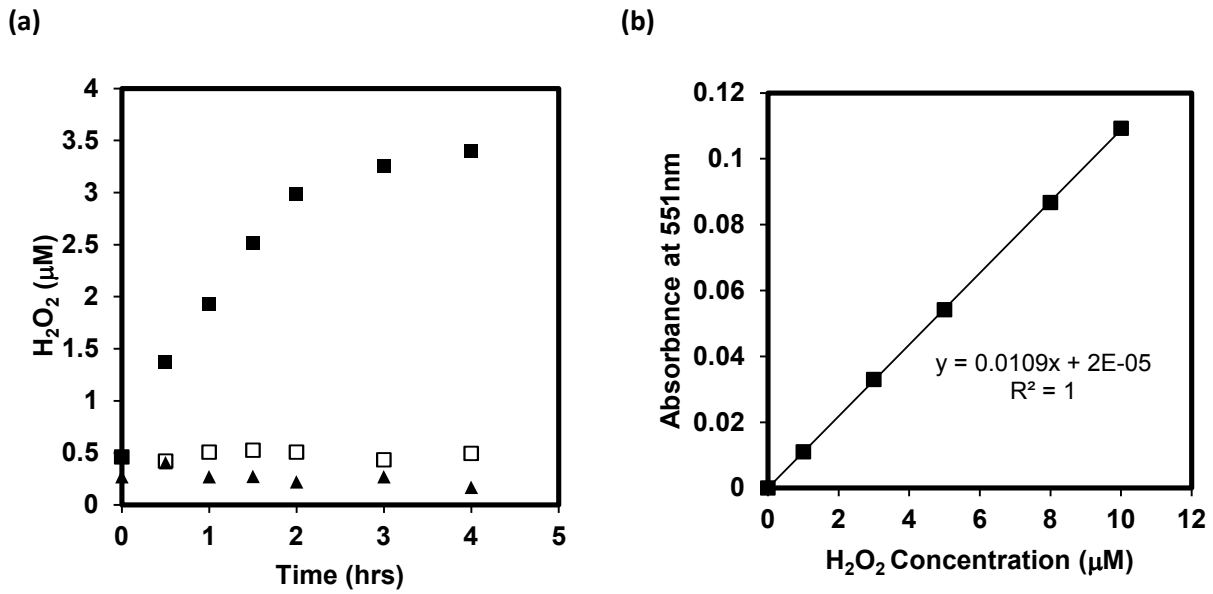

Figure 4. (a) Evidence for the increase in H_2O_2 concentration over time upon lamp light irradiation of GO at pH 7, by reacting the accumulated H_2O_2 with DPD through the HRP catalyzed reaction, producing the red colored DPD Würster dye product that absorbs light at 551 nm. All samples contain DPD and HRP, added after irradiating samples which contained 5 mg/L GO (■), or pure water (▲), or after incubating samples in the dark which contained 5 mg/L GO (□); and with the DPD and HRP added after filtering out the GO through 0.2 µm membrane filters. (b) The standard curve of H_2O_2 using DPD/HRP method.